# Superconducting Gap in the Hubbard Model and the Two-Gap Energy Scales of High-$T_c$ Cuprate Superconductors

M. Aichhorn,[1] E. Arrigoni,[2] Z. B. Huang,[3] and W. Hanke[1,*]

[1]*Institute for Theoretical Physics and Astrophysics, University of Würzburg, Am Hubland, 97074 Würzburg, Germany*
[2]*Institute of Theoretical Physics and Computational Physics, Graz University of Technology, Petersgasse 16, 8010 Graz, Austria*
[3]*Department of Physics, Hubei University, Wuhan 430062, People's Republic of China*

(Received 28 February 2007; published 17 December 2007)

Recent experiments (angle-resolved photoemission spectroscopy and Raman) suggest the presence of two distinct energy gaps in high-temperature superconductors (HTSC), exhibiting different doping dependences. The results of a variational cluster approach to the superconducting state of the two-dimensional Hubbard model are presented which show that this model qualitatively describes this gap dichotomy. The antinodal gap increases with less doping, a behavior long considered as reflecting the general gap behavior of the HTSC. On the other hand, the near-nodal gap does even slightly decrease with underdoping. An explanation of this unexpected behavior is given which emphasizes the crucial role of spin fluctuations in the pairing mechanism.

DOI: 10.1103/PhysRevLett.99.257002 PACS numbers: 74.20.−z, 71.10.Hf, 74.25.Jb, 74.72.−h

The celebrated pseudogap of high-temperature superconductors (HTSC) is widely believed to be intimately related to the microscopic pairing mechanism [1]. Early angle-resolved photoemission spectroscopy (ARPES) demonstrated that both the pseudogap and the superconducting gap below $T_c$ are consistent with the $d_{x^2-y^2}$ symmetry [2]. In addition, both gaps were found to have a more or less identical doping dependence, increasing when the doping was reduced [2,3]. This strongly supported a picture, where the pseudogap is a precursor to the $d_{x^2-y^2}$-superconducting (SC) state; i.e., the pseudogap smoothly evolves into the SC gap, when phase coherence of the pairs develops below $T_c$ [4–6]. Accordingly, there seemed to be only one energy scale in the system, namely, the magnitude of the gap in the antinodal region around $(\pi, 0)$. However, this picture has been challenged severely by Raman [7,8] and very recent ARPES investigations [9–11]: The experiments done below $T_c$ suggest two distinct energy gaps exhibiting different doping dependencies. While the gap near the antinodal $(\pi, 0)$ region was still found to strongly increase with decreasing doping, the other gap, identified from sharp (coherent) peaks near the nodal region, has a rather different doping dependence, i.e., does not increase with less doping. These surprising observations have been interpreted as a two-gap scenario, in which there are two energy scales, one corresponding to the near-nodal and one to the antinodal region around the Fermi surface (FS). Clearly, these recent findings pose also a substantial challenge to the microscopic theory.

In this Letter, we show that the two-dimensional (2D) Hubbard model accounts, at least qualitatively, for the observed different doping dependencies of the gaps near the nodal and near the antinodal regions. We suggest (see below) that this "two gaps" scenario can be naturally explained by the anisotropy of the $d$-wave coupling strength at the Fermi surface, which is related to the peaked structure of the spin-mediated pairing interaction $V_{\text{pairing}}$ around $\mathbf{Q}_{\text{AF}} = (\pi, \pi)$. These results emphasize the importance of spin fluctuations in the pairing mechanism for HTSC materials [12–16]. In addition, they support the premise that the physics of the intriguing HTSC materials should be contained in the 2D one-band Hubbard model. This premise has recently also obtained support from a variety of cluster calculations which reproduce the overall ground-state phase diagram of the HTSC as well as their single-particle excitation spectra [17–21].

Our main results, obtained by means of the variational cluster approach (VCA) [22,23], are shown in Figs. 2 and 3. In Fig. 2, we plot the SC gap near the antinodal and near the nodal point as a function of doping for the two-dimensional Hubbard model, whereby the $d$-wave factor has been divided off for a better comparison. The two gaps clearly behave differently as a function of doping, in agreement with the experimental findings [9–11]. While the antinodal gap increases, the nodal gap decreases with less doping. However, an analysis of our results in terms of the anomalous self-energy indicates that below $T_c$ there is only *one* gap mechanism. Both gaps are due to superconductivity, and there is no contribution from the normal self-energy, i.e., a remnant of the normal-state pseudogap.

As we show below, the so-called "two-gap" behavior can be explained by the doping dependence of the spin-fluctuation mediated pairing interaction $V_{\text{pairing}}(\mathbf{q})$ which displays a strongly peaked structure around $(\pi, \pi)$. The width $a$ of this structure is given by the inverse antiferromagnetic correlation length and, despite the reduction effect of vertex corrections, $a$ decreases with decreasing doping [24,25]. Because of the $d$-wave factor, the contribution to the superconducting gap $\Delta_{\text{SC}}(\mathbf{k})$ has a different dependence on the transfer momentum $\mathbf{q}$ of the effective interaction depending on whether $\mathbf{k}$ is close to the nodal or antinodal region. This fact, connected with the doping depen-

 

dence of the peak structure of $V_{\text{pairing}}$ around $(\pi, \pi)$ accounts for both the qualitatively different doping dependencies of the gaps near $(\pi, 0)$ or near $(\frac{\pi}{2}, \frac{\pi}{2})$, as well as for the deviation of the SC gap from the nearest-neighbor $d$-wave form $\cos k_x - \cos k_y$ as observed in experiments [9–11,26].

Our results are obtained on the basis of two numerical techniques, which are appropriate for the treatment of strongly correlated materials, namely, the VCA [22,23] and a quantum Monte Carlo (QMC) cluster solution [24,25]. The VCA is based on the self-energy functional theory, which was proposed and applied by Potthoff *et al.* [27–29]. It provides a variational scheme to use dynamical information from an exactly solvable "reference" system (in the VCA an isolated cluster) to go to the infinite-sized lattice fermion system at low temperatures and at $T = 0$, in particular. The 2D Hubbard model is given by

$$H = \sum_{ij,\sigma} t_{ij} c^{\dagger}_{i\sigma} c_{j\sigma} + U \sum_{i} n_{i\uparrow} n_{i\downarrow}, \qquad (1)$$

where $t_{ij}$ denote hopping matrix elements, $n_{i\uparrow}$ denote the density at site $i$ with spin "↑," and $U$ denotes the local Coulomb repulsion. Its ground-state phase diagram was calculated within the VCA by Sénéchal *et al.* [18] and by our group [19,29,30]. For the cluster size used in the VCA (up to 10 site clusters solved by a Lanczos technique), the $T = 0$ phase diagram of the Hubbard model in Eq. (1), with hopping terms up to third-nearest neighbors, correctly reproduces salient features of the HTSC, such as the antiferromagnetic (AF) and superconducting ground states in doping ranges, which are qualitatively in agreement with electron- and hole-doped cuprates.

Also the single-particle excitations agree with earlier QMC data [31] and with the main features observed in experiment [32]: clear signatures of the Mott gap, as well as the "coherent" quasiparticle band of width $J$ (≡magnetic exchange) and the "incoherent" lower and upper Hubbard bands are identified.

In Fig. 1(b) we show a typical Fermi surface for the underdoped case at $x = 0.07$ hole doping, obtained from the weight of the VCA single-particle spectral function at zero energy, $A(\mathbf{k}, \omega = 0)$. The largest weight is found near the nodal direction, marked by $N$ in Fig. 1, which corresponds to the "Fermi arc." The weak features suggesting a splitting of the Fermi surface when going to the antinodal region are due to the finite cluster used as a reference system. Accordingly, we measure the gap in the coherent region around the node between line 0 and line 6 in Fig. 1(b), and at the antinodal region marked by AN in Fig. 1.

In Fig. 2(a) we plot the (normalized) SC gaps $\Delta_0 \equiv 2\Delta_{\mathbf{k}}/(\cos k_x - \cos k_y)$ near the nodal and near the antinodal Fermi points as a function of doping $x$. As in experiment, the amplitude of the $d$-wave gap in the nodal region *decreases* when driving the system from the optimal doped into the underdoped region, while it *increases* in the antinodal region. The different doping dependences for the

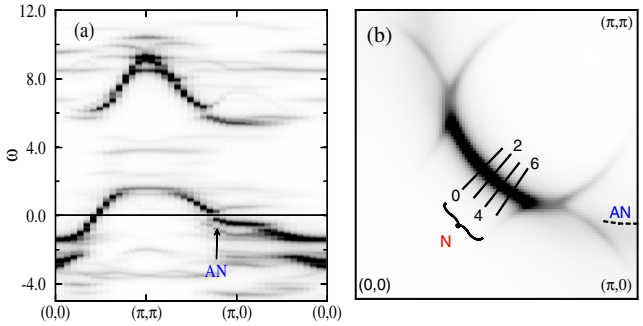


FIG. 1 (color online). (a) Spectral function of the Hubbard model for $U = 8t$, $t' = -0.3t$, and $x = 0.07$ hole doping, calculated with the VCA on a $3 \times 3$ cluster in the SC symmetry-broken phase. The arrow denotes the antinodal (AN) region. (b) The corresponding Fermi surface. The antinodal region is marked by AN (blue), the nodal region by N (red). Solid lines indicate the momentum scans, along which the gap is determined. Numbers refer to Fig. 2.

nodal and the antinodal regions correspond to the two different energy scales observed in photoemission experiments. From the figure it is clear that $\Delta(\mathbf{k})$ cannot be described by a simple nearest-neighbor $d$-wave form near both the nodal and the antinodal point, especially for low dopings. On the other hand, our plot of $\Delta(\mathbf{k})$ displayed in Fig. 2(b) shows that in an extended region around the nodal point the gap retains its nearest-neighbor $d_{x^2-y^2}$ form; see also the inset of Fig. 2(b). This latter finding is again in accordance with experiment [see the inset of Fig. 3(a) in Ref. [9] ].

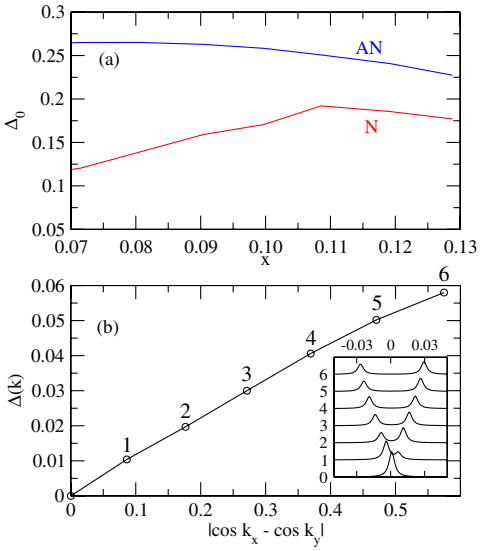


FIG. 2 (color online). (a) "Normalized" SC gap $\Delta_0 \equiv 2\Delta_{\mathbf{k}}/(\cos k_x - \cos k_y)$ for $\mathbf{k}$ near the antinodal (AN) and near the nodal FS point (N) as a function of doping for the Hubbard model (parameters are given in the text). (b) SC gap as a function of the $d$-wave factor $(\cos k_x - \cos k_y)$ on the Fermi arc for $x = 0.07$ hole doping. The numbers correspond to the momentum scans marked in Fig. 1. Inset: $A(\mathbf{k}, \omega)$ in a small window around the FS for points 0 to 6.

For the understanding of this behavior it is first of all interesting to find out whether the gap originates only from one mechanism, related to superconductivity, or if there are competing mechanisms producing different gaps. In our calculation, we can address this question in the following way. In matrix-Nambu formalism the Dyson equation reads (see also Ref. [33])

$$G^{-1}_{\alpha\beta}(\boldsymbol{Q},\omega) = \begin{pmatrix} \omega - T_{\alpha\beta}(\boldsymbol{Q}) - \Sigma^{\mathrm{no}}_{\alpha\beta}(\omega) & -\Sigma^{\mathrm{sc}}_{\alpha\beta}(\omega) \\ -\Sigma^{\mathrm{sc}}_{\alpha\beta}(\omega) & \omega + T_{\alpha\beta}(\boldsymbol{Q}) + \Sigma^{\mathrm{no}^*}_{\alpha\beta}(-\omega) \end{pmatrix}, \tag{2}$$

with $T_{\alpha\beta}(\boldsymbol{Q})$ the hopping matrix, and $\alpha$, $\beta$ being the quantum numbers within the reference system, i.e., the cluster sites. After the variational opimization procedure, we set the SC-related parts of the self-energy $\Sigma^{\mathrm{sc}}_{\alpha\beta}$ to zero and evaluate the corresponding spectral function. By comparing the left (full SC solution) and the middle panel ($\Sigma^{\mathrm{sc}}_{\alpha\beta} = 0$) in Fig. 3, one can clearly see that the gap around $(\pi, 0)$ is *only* due to $\Sigma^{\mathrm{sc}}_{\alpha\beta}$, and there are no signatures of a remaining underlying pseudogap produced by a mechanism different from superconductivity. Figure 3 shows results for $x = 0.07$ hole doping, but we have checked that this behavior is the same in the whole doping range under investigation.

Since it is known that above $T_c$ the Hubbard model shows a pseudogap behavior [20,31], we also compare our superconducting results with "normal"-state solutions, where we do not allow for $U(1)$ symmetry breaking in the variational procedure. The right panel of Fig. 3 shows that in this solution there is indeed a pseudogap. Interestingly, this pseudogap increases by lowering the doping and, thus, shows a doping dependence in qualitative agreement with finite-$T$ QMC simulations [31] and also ARPES experiments, identifying the pseudogap above $T_c$ with the leading edge features near $(\pi, 0)$ [2,3,11]. Our calculation is at $T = 0$. However, taking all the above results together, they indicate that the breaking of the $U(1)$ symmetry destroys the "normal-state" origin of the pseudogap, and the gap "below $T_c$" is due only to superconductivity.

What is the physical reason for the different doping dependence of the nodal and antinodal gap? We argue that this behavior is related to the anisotropy of the $d$-wave coupling strength at the Fermi surface in combination with the doping dependence of the peaked structure of the spin-fluctuation mediated pairing interaction including full vertex corrections. With a previously developed formalism [25] based on QMC calculations, this effective pairing strength including the renormalization of the density of states can be calculated. Results obtained for the $t$-$t'$-$U$ (2D) Hubbard model showed that the effective pairing interaction $V_{\mathrm{pairing}} = v(\mathbf{k}, \mathbf{q})$ mediated by AF spin fluctuations is significantly influenced and reduced due to vertex corrections, but it clearly remains peaked around $(\pi, \pi)$ [24,25]. This latter fact is, of course, well known from earlier unrenormalized random-phase approximation calculations. Most importantly, for transfer momenta $\mathbf{q}$ near $(\pi, \pi)$, the effective interaction (evaluated at the lowest Matsubara frequency) sharply increases with decreasing doping; see Fig. 4. In contrast, for transfer momenta away from $(\pi, \pi)$, such as $\mathbf{q} = (\pi, 0)$, $v(k, q)$ shows only at best a very weak increase with doping.

Although HTSC materials are clearly strongly correlated, our argument can be understood qualitatively by means of a simple BCS gap equation for $\Delta(\mathbf{k}_F)$ at the Fermi point $\mathbf{k}_F$:

$$\Delta(\mathbf{k}_F) = -\int \frac{d^2k'}{(2\pi)^2} v(\mathbf{k}' - \mathbf{k}_F) \frac{\Delta(\mathbf{k}')}{E(\mathbf{k}')}. \tag{3}$$

Here, $E(\mathbf{k}') = \sqrt{\xi^2_{\mathbf{k}'} + \Delta(\mathbf{k}')^2}$, $\xi_{\mathbf{k}'}$ being the single-particle energy measured from the chemical potential. After integrating over momenta perpendicular to the Fermi surface in a thin energy shell of width $\Omega \propto J \ll t$, for $\Delta \ll \Omega$ one obtains

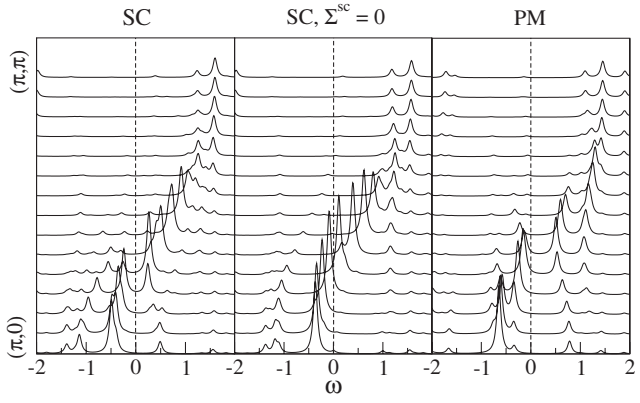


FIG. 3. Spectral function from $(\pi, 0)$ to $(\pi, \pi)$ at $h = 0.07$ doping. Left: $A(\boldsymbol{k}, \omega)$ in the SC broken phase. Middle: SC phase, but $\Sigma^{\mathrm{sc}} = 0$ (see the text). Right: Paramagnetic solution.

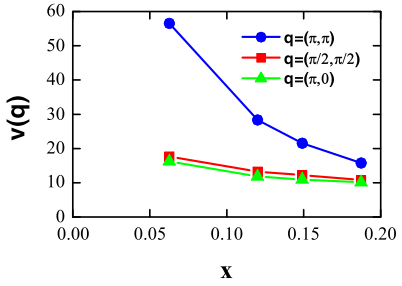


FIG. 4 (color online). The doping dependence of $v(q)$ at $q = (\pi, \pi)$, $(\frac{\pi}{2}, \frac{\pi}{2})$, and $(\pi, 0)$ for $U = 8t$, calculated with the QMC method on an $8 \times 8$ cluster for inverse temperature $\beta = 2.5t^{-1}$. Notice that the interaction hardly depends on the fermionic momentum $\mathbf{k}$, so only the dependence on $\mathbf{q}$ is shown for $\mathbf{k} = (-\pi, 0)$.

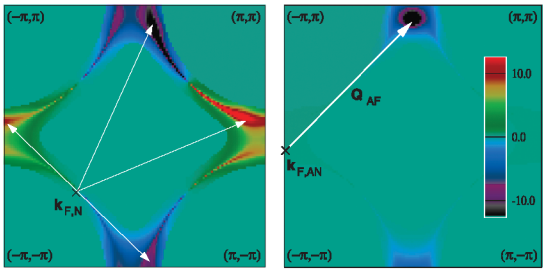


FIG. 5 (color). Contributions to the gap $\Delta(\mathbf{k}_F)$ in Eq. (3) as a function of $\mathbf{k}'$, divided by the $d$-wave factor $\cos(k_{F,x}) - \cos(k_{F,y})$ for normalization reasons. Typical parameters have been used, $\mu = -1.0t$, $t' = -0.3t$. Left: Fermi momentum $\mathbf{k}_{F,N}$ near the nodal direction. Arrows indicate transfer vectors with large weights. Right: Fermi momentum $\mathbf{k}_{F,\mathrm{AN}}$ near the antinodal direction. The arrow is the AF momentum $\mathbf{Q}_{\mathrm{AF}}$. The color scale for both plots is given in the right plot.

$$\Delta(\mathbf{k}_F) \approx -\int d\hat{\mathbf{k}}'_F n(\mathbf{k}'_F) v(\mathbf{k}'_F - \mathbf{k}_F) \Delta(\mathbf{k}'_F) \log \frac{\Omega}{|\Delta(\mathbf{k}'_F)|}, \tag{4}$$

with $n(\mathbf{k}'_F)$ the density of states per unit area of the FS at $\mathbf{k}'_F$. The integral in Eq. (4) extends over the Fermi surface $d\hat{\mathbf{k}}'_F$, the log comes from the integration of the energy denominator, and we have exploited the fact that $v$ depends mainly on the momentum transfer $\mathbf{q} = \mathbf{k}'_F - \mathbf{k}_F$. For $\mathbf{k}_F$ near the antinodal point $(\pi, 0)$ the strongest contribution [normalized to the value of $v(\mathbf{q})$] comes from $\mathbf{k}'_F$ near the two antinodal points $(0, \pi)$ and $(0, -\pi)$, i.e., for $\mathbf{q} = \mathbf{k}_F - \mathbf{k}'_F$ near $(\pi, \pi)$. It is thus clear from the behavior of $v(\mathbf{q})$ as a function of doping shown in Fig. 4 that one expects $\Delta[\mathbf{k}_F \sim (\pi, 0)]$ to decrease fast with increasing doping. On the other hand, for $\mathbf{k}_F$ around the nodal point $(\frac{\pi}{2}, \frac{\pi}{2})$, the contribution for other nodal points cannot be strong since it is suppressed by the nodes in $\Delta(\mathbf{k}'_F)$. As a result, the strength of the SC gap is controlled by $v(\mathbf{q})$ at momenta away from $\mathbf{q} = (\pi, \pi)$. In order to eludicate this point, we plot in Fig. 5 the contributions to the integral Eq. (3) for typical parameters $\mu = -1.0t$, $t' = -0.3t$, which show exactly the behavior described above. Hence, the behavior of $v(\mathbf{q})$ for $\mathbf{q}$ away from $(\pi, \pi)$ shown in Fig. 4 provides the physical reason for which the SC gap at the nodal point does not increase with decreasing doping [33,34].

Summarizing, we have shown that VCA calculations within the $t$-$t'$-$U$ Hubbard model qualitatively reproduce the different doping dependences of the superconducting gap recently seen in experiments. When going to lower hole dopings, the gap on the Fermi arc, near the nodal region, *decreases,* whereas the gap near the antinode *increases*. Moreover, we have shown that there is no indication in our results for a two-gap scenario with distinct superconducting and pseudogap below $T_c$. Instead, we found that obviously the SC gap in the symmetry-broken solution absorbs the normal-state pseudogap, resulting in a ''one-gap'' scenario with only a SC gap below $T_c$ exhibiting a more complicated structure in momentum space. This more complicated structure is shown to be naturally explained in terms of a spin-mediated pairing mechanism.

We thank Z.-X. Shen, A. V. Chubukov, and E. Schachinger for constructive discussions, and, in particular, D. J. Scalapino for his comments on the SC self-energy. This work was supported by the Deutsche Forschungsgemeinschaft, Grant No. FOR 538, and by the Austrian science fund (FWF Project No. P18551-N16). Z. B. H. was supported in part by NSFC Grant No. 10674043.

*hanke@physik.uni-wuerzburg.de

[1] See, e.g., T. Timusk and B. W. Statt, Rep. Prog. Phys. **62**, 61 (1999).
[2] A. G. Loeser *et al.*, Science **273**, 325 (1996).
[3] H. Ding *et al.*, Nature (London) **382**, 51 (1996).
[4] Y. J. Uemura *et al.*, Phys. Rev. Lett. **62**, 2317 (1989).
[5] M. Randeria *et al.*, Phys. Rev. Lett. **62**, 981 (1989).
[6] V. J. Emery and S. A. Kivelson, Nature (London) **374**, 434 (1995).
[7] M. Opel *et al.*, Phys. Rev. B **61**, 9752 (2000).
[8] M. Le Tacon *et al.*, Nature Phys. **2**, 537 (2006).
[9] K. Tanaka *et al.*, Science **314**, 1910 (2006).
[10] T. Kondo *et al.*, Phys. Rev. Lett. **98**, 267004 (2007).
[11] M. Hashimoto *et al.*, Phys. Rev. B **75**, 140503(R) (2007).
[12] For a review on the spin-fluctuation mechanism, see, e.g., A. Abanov, A. V. Chubukov, and J. Schmalian, Adv. Phys. **52**, 119 (2003).
[13] N. F. Berk and J. R. Schrieffer, Phys. Rev. Lett. **17**, 433 (1966).
[14] D. J. Scalapino *et al.*, Phys. Rev. B **34**, 8190 (1986).
[15] V. J. Emery, Synth. Met. **13**, 21 (1986).
[16] A. J. Millis *et al.*, Phys. Rev. B **42**, 167 (1990).
[17] T. A. Maier *et al.*, Phys. Rev. Lett. **95**, 237001 (2005).
[18] D. Sénéchal *et al.*, Phys. Rev. Lett. **94**, 156404 (2005).
[19] M. Aichhorn *et al.*, Phys. Rev. B **74**, 024508 (2006).
[20] A. Macridin *et al.*, Phys. Rev. Lett. **97**, 036401 (2006).
[21] B. Kyung *et al.*, Phys. Rev. B **73**, 165114 (2006).
[22] M. Potthoff *et al.*, Phys. Rev. Lett. **91**, 206402 (2003).
[23] C. Dahnken *et al.*, Phys. Rev. B **70**, 245110 (2004).
[24] Z. B. Huang *et al.*, Europhys. Lett. **71**, 959 (2005).
[25] Z. B. Huang *et al.*, Phys. Rev. B **74**, 184508 (2006).
[26] J. Mesot *et al.*, Phys. Rev. Lett. **83**, 840 (1999).
[27] M. Potthoff, Eur. Phys. J. B **36**, 335 (2003).
[28] M. Potthoff, Eur. Phys. J. B **32**, 429 (2003).
[29] M. Aichhorn *et al.*, Phys. Rev. B **74**, 235117 (2006).
[30] M. Aichhorn and E. Arrigoni, Europhys. Lett. **72**, 117 (2005).
[31] R. Preuss *et al.*, Phys. Rev. Lett. **79**, 1122 (1997).
[32] A. Damascelli *et al.*, Rev. Mod. Phys. **75**, 473 (2003).
[33] M. Civelli *et al.*, arXiv:0704.1486.
[34] The fact that for strongly peaked pairing the gap deviates from the simple nearest-neighbor form was first discussed by A. Abanov *et al.*, Europhys. Lett. **54**, 488 (2001).
[35] We stress that this BCS calculation has been done in order to provide a first qualitative understanding of our theoretical results shown in Fig. 2. We have checked that this behavior is also obtained within an Eliashberg calculation.